Available online at www.sciencedirect.com
ScienceDirect
Journal of Sound and Vibration 310 (2008) 38–57
JOURNAL OF SOUND AND VIBRATION
www.elsevier.com/locate/jsvi

Dynamic analysis of conical shells conveying fluid

D. Senthil Kumar, N. Ganesan*

Machine Dynamics Laboratory, Department of Applied Mechanics, IIT Madras 600 036, India

Received 25 June 2007; accepted 3 July 2007

Abstract

A formulation, based on the semi-analytical finite element method, is proposed for elastic conical shells conveying fluids. The structural equations are based on the shell element proposed by Ramasamy and Ganesan [Finite element analysis of fluid-filled isotropic cylindrical shells with constrained viscoelastic damping, *Computers & Structures* 70 (1998) 363–376] while the fluid model is based on velocity potential formulation used by Jayaraj et al. [A semi-analytical coupled finite element formulation for composite shells conveying fluids, *Journal of Sound and Vibration* 258(2) (2002) 287–307]. Dynamic pressure acting on the walls is derived from Bernoulli's equation. By imposing the requirement that the normal component of velocity of the solid and fluid are equal leads to fluid–structure coupling. The computer code developed has been validated using results available in the literature for cylindrical shells conveying fluid. The study has been carried out for conical shells of different cone angles and for boundary condition like clamped–clamped, simply supported and clamped free. In general, instability occurs at a critical fluid velocity corresponding to the shell circumferential mode with the lowest natural frequency. Critical fluid velocities are lower than that of equivalent cylindrical shells. This result holds good for all boundary conditions.

1. Introduction

The dynamics of pipes conveying fluid has been extensively investigated [1,2] as seen from the comprehensive review paper by Païdoussis and Li [3] and the recent book by Païdoussis [4]. However, most of the investigations have been based on analytical models for the structure and/or fluid. Shells conveying fluids have attracted relatively less attention. Ramasamy and Ganesan [1] studied the vibration characteristics of fluid-filled shells with a constrained viscoelastic layer based on Wilkins theory [5]. However, they did not consider fluid flow. Selman and Lakis [6] have developed a theory for the determination of the effects of flowing fluid on the vibration characteristics of an open anisotropic cylindrical shell submerged in fluid and subjected simultaneously to an external and internal flow. They have used an analytical formulation to solve the fluid part. Chang and Chiou [7] studied the natural frequencies and critical velocities of laminated circular cylindrical shells with fixed ends conveying fluid using a hybrid

*Corresponding author.
E-mail address: nganesan@iitm.ac.in (N. Ganesan).

0022-460X/$ - see front matter © 2007 Elsevier Ltd. All rights reserved.
doi:10.1016/j.jsv.2007.07.020

FE/analytical method. They used a Mindlin-type first-order transverse shear deformable cylindrical shell theory for the structure and an analytical method for the fluid. For complex piping geometry, analytical techniques cannot be used.

A number of investigators have proposed finite element formulations for fluid flow problems. For instance, Everstine [8] proposed a velocity potential formulation for a symmetric finite element solution of transient wave propagation problems. Lakis et al. [9] have carried out dynamic analysis of anisotropic fluid-filled conical shells. Even though their formulation includes the influence of flow terms their study is limited to quiescent fluid. From the literature survey, it is found that there is no work dealing with dynamic analysis of conical shells conveying fluid. Since conical shells are axisymmetric a semi-analytical finite element formulation would be more useful. It is noted from the literature that pipe instability occurs predominantly in the bending mode (first circumferential mode, $m = 1$). In contrast the behavior of a conical shell may not be similar to that of a pipe. The main objective of this paper is to bring out the difference between the behavior cylindrical and conical shells conveying fluid. Hence in the present study, an analysis is carried out for different boundary conditions of the conical shell. In addition the paper aims to establish a relation between the instability and the circumferential modes of the shell as a function of boundary conditions, geometry.

2. Finite element formulation

2.1. Structure

The (s, θ, z) coordinate system for general shells of revolution is illustrated in Fig. 1. By setting the value of the principal radius of curvature R_ϕ equal to infinity and the other principal radius of curvature R_θ equal to a finite radius equal to $r/\sin\phi$, where r is the radius that vary linearly along the length depending upon the vertex angle (α), then the geometry resembles a conical shell as illustrated in Fig. 2. The displacements according to the first-order shear deformation theory are expressed as

$$u(s,\theta,z,t) = u_o(s,\theta,t) + z\psi_s(s,\theta,t), \tag{1a}$$

$$v(s,\theta,z,t) = v_o(s,\theta,t) + z\psi_\theta(s,\theta,t), \tag{1b}$$

$$w(s,\theta,z,t) = w_o(s,\theta,t), \tag{1c}$$

where u_o, v_o, w_o are displacement of mid-surface along the s, θ and z directions and ψ_s and ψ_θ are rotations of the normal to the mid-surface along s and θ axes, respectively. In the semi-analytical method, the generalized displacement field is assumed to depend in the circumferential direction and expressed using

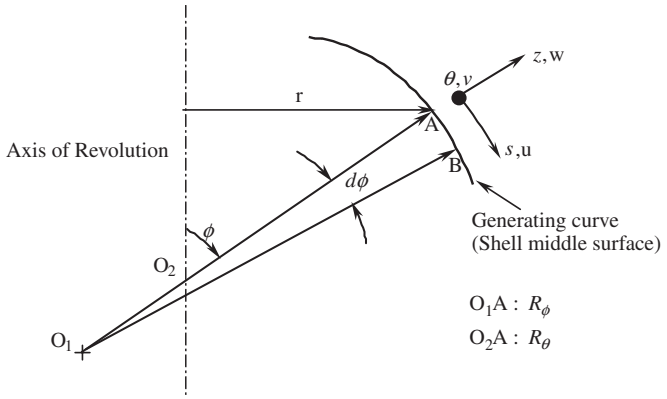

Fig. 1. General shell of revolution.

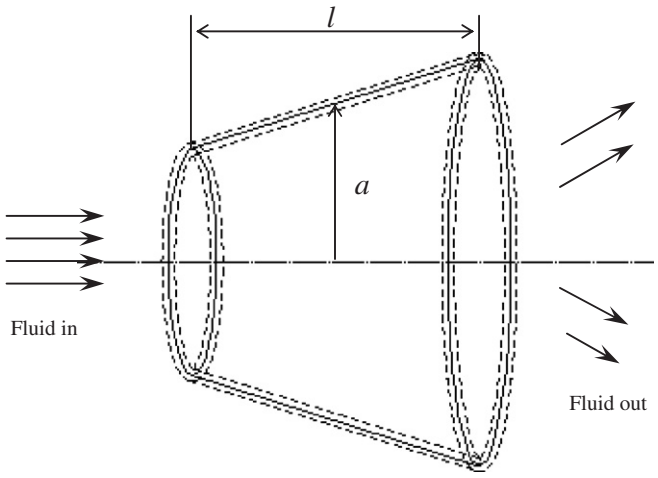

Fig. 2. Geometry of conical shell.

Fourier-series as follows:

$$\begin{Bmatrix} u_o \\ v_o \\ w_o \\ \psi_s \\ \psi_\theta \end{Bmatrix} = \sum_{m=0}^{\infty} \begin{bmatrix} \cos m\theta & 0 & 0 & 0 & 0 \\ 0 & \sin m\theta & 0 & 0 & 0 \\ 0 & 0 & \cos m\theta & 0 & 0 \\ 0 & 0 & 0 & \cos m\theta & 0 \\ 0 & 0 & 0 & 0 & \sin m\theta \end{bmatrix} \begin{Bmatrix} u_{om} \\ v_{om} \\ w_{om} \\ \psi_{sm} \\ \psi_{\theta m} \end{Bmatrix}, \tag{2}$$

where 'm' indicates the harmonic number (or circumferential mode number).

The semi-analytical finite element formulation for general shells of revolution is based on the first-order shear deformation theory. The structural stiffness matrix is derived from the strain energy, Ramasamy and Ganesan [1].

The kinematic relation for a doubly curved shell of revolution in the (s, θ, Z) coordinate based on FSDT are as follows:

$$\varepsilon_{ss} = \frac{1}{A_1}(\varepsilon^o_{ss} + z\kappa^1_s), \quad \gamma_{\theta z} = \frac{1}{A_2}\gamma^o_{\theta z}, \tag{3a,b}$$

$$\varepsilon_{\theta\theta} = \frac{1}{A_2}(\varepsilon^o_{\theta\theta} + z\kappa^1_\theta), \quad \gamma_{sz} = \frac{1}{A_1}\gamma^o_{sz}, \tag{3c,d}$$

$$\gamma_{s\theta} = \frac{1}{A_1}\frac{1}{A_2}(\gamma^o_{s\theta} + z\kappa^1_{s\theta}), \tag{3e}$$

where

$$\frac{1}{A_1} = \frac{1}{(1 + (z/R_\phi))} \quad \text{and} \quad \frac{1}{A_2} = \frac{1}{(1 + (z/R_\theta))}$$

in the above equations R_ϕ and R_θ are the principle radii of curvature of the shell as illustrated in Fig. 1 and z is the thickness in z-direction. The total strains are denoted as $\varepsilon_{ss}, \varepsilon_{\theta\theta}, \gamma_{\theta z}, \gamma_{sz}$ and $\gamma_{s\theta}$; which comprise of the normal strains and the shear strains:$\varepsilon^o_{ss}, \varepsilon^o_{\theta\theta}, \gamma^o_{\theta z}, \gamma^o_{sz}, \gamma^o_{s\theta}$, referred to mid-surface and $\kappa^1_s, \kappa^1_\theta, \kappa^1_{s\theta}$, the change in curvature of the mid-surface. For a general shell of revolution these strain components are given below:

$$\varepsilon^o_{ss} = \frac{\partial u_o}{\partial s} + \frac{w}{R_\phi}; \quad \varepsilon^o_{\theta\theta} = \frac{1}{r}\frac{\partial v_o}{\partial \theta} + \frac{u_o}{r}\cos\,\phi + \frac{w_o}{r}\sin\,\phi, \tag{4a,b}$$

$$\gamma^o_{\theta z} = \phi_\theta - \frac{v_0}{r}\sin\,\phi + \frac{1}{r}\frac{\partial w_o}{\partial \theta}; \quad \gamma^o_{s\theta} = \frac{1}{r}\frac{\partial u_o}{\partial \theta} + \frac{\partial v_o}{\partial s} - \frac{v_o}{r}\cos\,\phi, \tag{4c,d}$$

$$\gamma^o_{sz} = \phi_s - \frac{u_o}{R_\phi} + \frac{\partial w_o}{\partial s}, \tag{4e}$$

$$\kappa^1_s = \frac{\partial \phi_s}{\partial s}; \quad \kappa^1_\theta = \frac{1}{r}\frac{\partial \phi_\theta}{\partial \theta} + \frac{\phi_s}{r}\cos\,\phi, \tag{4f}$$

$$\kappa^1_{s\theta} = \frac{1}{r}\frac{\partial \phi_s}{\partial \theta} + \frac{\partial \phi_\theta}{\partial s} - \frac{\phi_\theta}{r}\cos\,\phi + \frac{\sin\,\phi}{r}\frac{\partial v_o}{\partial s} + \frac{1}{R_\phi r}\frac{\partial u_o}{\partial \theta} - \frac{v_o}{R_\phi r}\cos\,\phi. \tag{4g}$$

Accordingly, it follows that the strain vector will comprise of

$$\boldsymbol{\varepsilon}^{\mathbf{T}} = \left\{\varepsilon^0_{ss}\varepsilon^0_{\theta\theta}\gamma^0_{s\theta}\kappa^1_s\kappa^1_\theta\kappa^1_{s\theta}\gamma^0_{sz}\gamma^0_{\theta z}\right\} \quad \text{or} \quad \varepsilon = \left\{\begin{array}{c}\boldsymbol{\varepsilon}^o\\ \boldsymbol{\kappa}^1\\ \boldsymbol{\gamma}^o\end{array}\right\}, \tag{5}$$

where

$$(\boldsymbol{\varepsilon}^o)^{\mathrm{T}} = \{\,\varepsilon^o_{ss} \quad \varepsilon^o_{\theta\theta} \quad \gamma^o_{s\theta}\,\}, \quad (\boldsymbol{\kappa}^1)^{\mathrm{T}} = \{\,\kappa^1_s \quad \kappa^1_\theta \quad \kappa^1_{s\theta}\,\} \quad \text{and} \quad (\boldsymbol{\gamma}^o)^{\mathrm{T}} = \{\,\gamma^o_{sz} \quad \gamma^o_{\theta z}\,\}. \tag{6}$$

In shell analyses, it is generally convenient to deal with the stress resultants and moment resultants rather than directly the stresses. Thus when each component of the stress vector, $\boldsymbol{\sigma}^{\mathrm{T}} = \{\,\sigma_{ss} \quad \sigma_{\theta\theta} \quad \tau_{\theta z} \quad \tau_{sz} \quad \tau_{s\theta}\,\}$, integrated over the thickness of the shell will comprise of the stress resultants and moment resultants, and these are referred through the generalized stress vector represented as

$$\bar{\mathbf{N}}^* = \left\{\begin{array}{c}\bar{\mathbf{N}}\\ \bar{\mathbf{M}}\\ \bar{\mathbf{Q}}\end{array}\right\}, \tag{7}$$

where

$$\bar{\mathbf{N}}^{\mathrm{T}} = \left\{\,N_{SS} \quad N_{\theta\theta} \quad N_{S\theta}\,\right\}; \ \bar{\mathbf{M}}^{\mathrm{T}} = \left\{\,M_{SS} \quad M_{\theta\theta} \quad M_{S\theta}\,\right\}; \ \bar{\mathbf{Q}}^{\mathrm{T}} = \left\{\,Q_{SS} \quad Q_{\theta\theta}\,\right\}. \tag{8}$$

It is clear that from Fig. 1, that by setting the value of the principal radius of curvature R_ϕ equal to infinity,ϕ equal to $(90^\circ-\alpha)$ and the other principal radius of curvature R_θ equal to a finite radius equal to $r/\sin\phi$ where r is the radius that vary linearly along the length depending upon the vertex angle (α), then the geometry resembles a conical shell. Considering these simplifications, the general strain displacement relations are used to formulate the stiffness and mass matrix.

A three-node isoparametric line element is used along the s-coordinate to generate the finite element mesh for the conical shell (see Fig. 3). Each node has five degrees of freedom (dofs). The displacements parameters associated with the element are

$$\mathbf{d}^{\mathrm{T}}_e = \{u_1, v_1, w_{1,}\psi_{s1}, \psi_{\theta 1}, u_2, v_2, w_{2,}\psi_{s2}, \psi_{\theta 2}, u_3, v_3, w_3, \psi_{s3}, \psi_{\theta 3}\}. \tag{9}$$

The subscripts 1–3 stand for the three nodes of the element. The shape functions N_i in terms of the isoparametric axial coordinate $\beta = \bar{s}/l$ (where $\bar{s}$ denotes the distance of a point on the element along the s-coordinate and l is the length of the element) are given by

$$N_1 = \frac{(\beta^2-\beta)}{2}, \quad N_2 = (1-\beta^2) \quad \text{and} \quad N_3 = \frac{(\beta^2+\beta)}{2}. \tag{10}$$

Displacement within the element are interpolated from nodal dof vector $\mathbf{d}_e$

$$\mathbf{u} = \mathbf{N}\mathbf{d}_e, \tag{11}$$

where $\mathbf{u}^{\mathrm{T}} = \{\,u \quad v \quad w\,\}$. Strains are obtained from displacements by differentiation. Thus $\varepsilon = [\partial]\mathbf{u}$ yields $\varepsilon = \mathbf{B}^*\mathbf{d}_e$, where $\mathbf{B}^* = [\partial]\mathbf{N}$ and $[\partial]$ is the differential operator matrix given by the strain displacement relations.

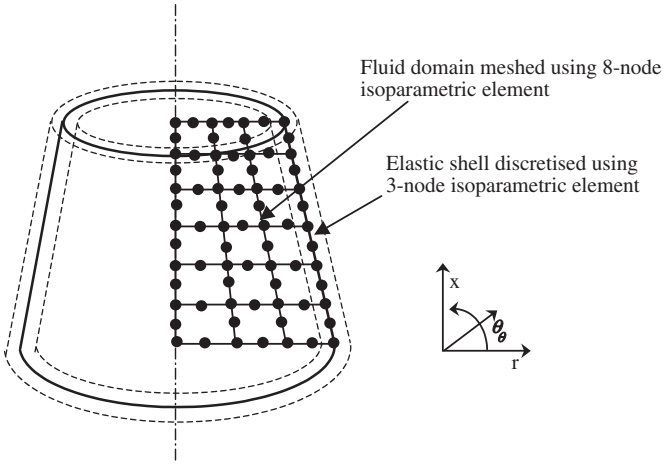

Fig. 3. Discretization of structure (3-noded isoparametric line and fluid part 8-noded isoparametric element).

The stress strain relation for a shell lamina can be expressed as, $\boldsymbol{\sigma} = \overline{\overline{\mathbf{Q}}}^{*}\varepsilon$, where $\overline{\overline{\mathbf{Q}}}^{*} = \mathbf{T}^{-1}\overline{\overline{\mathbf{Q}}}\mathbf{T}^{-\mathrm{T}}$ represents the transformed reduced stiffness where $\mathbf{T}^{-1}$ is the coordinate transformation matrix from the material coordinates to shell coordinates, $\overline{\overline{\mathbf{Q}}}$ denotes the reduced stiffness. Reader can refer to Jones [10] and Decolon [11] for details of constitutive matrix. In the case of shell analysis where one refers the strain with respect to mid-surface, then the generalized stresses are related through the integrated shell stiffness as follows:

$$\begin{Bmatrix} \bar{\mathbf{N}} \\ \bar{\mathbf{M}} \\ \bar{\mathbf{Q}} \end{Bmatrix} = \begin{bmatrix} \mathbf{A} & \mathbf{B} & 0 \\ \mathbf{B} & \mathbf{D} & 0 \\ 0 & 0 & \mathbf{F} \end{bmatrix} \begin{Bmatrix} \boldsymbol{\varepsilon}^{O} \\ \boldsymbol{\kappa}^{1} \\ \boldsymbol{\gamma}^{O} \end{Bmatrix} \tag{12}$$

or $\bar{\mathbf{N}}^{*} = \bar{\mathbf{D}}\,\boldsymbol{\varepsilon}$, the integrated transformed reduced shell stiffness are obtained as follows:

$$(A_{ij}, B_{ij}, D_{ij}, F_{ij}) = \int_{-(h/2)}^{+(h/2)} \bar{Q}_{ij}(1, z, z^2, z^3)\,\mathrm{d}z, \tag{13}$$

where $i = 1, 2$ and 6 and $j = 1, 2$ and 6. (*Note*: $\bar{Q}_{ij}$, tensorial notation, and $\overline{\overline{\mathbf{Q}}}$, matrix notation, mean the same). A_{ij} are extensional stiffness, B_{ij} are the bending–extensional coupling stiffness, D_{ij} are bending stiffness and are the thickness shear stiffness. The stiffness matrix is obtained from the strain energy F_{ij} as

$$U_1 = \tfrac{1}{2}\mathbf{d}_e^{\mathrm{T}}\mathbf{k}_e\mathbf{d}_e, \tag{14}$$

where $\mathbf{k}_e$ is the elemental stiffness matrix corresponding to the mth harmonic and is computed as follows:

$$\mathbf{k}_e = \int_A \mathbf{B}^{*^{\mathrm{T}}}\,\bar{\mathbf{D}}\,\mathbf{B}^{*} r\,\mathrm{d}s\,\mathrm{d}\theta, \tag{15}$$

where $\mathbf{B}^{*}$ is the strain–displacement matrix of the shell. The element stiffness matrix is assembled using standard assembly procedure in finite element analysis to obtain the global stiffness matrix, $\mathbf{K}^{uu} = \Sigma\mathbf{k}_e$. Owing to orthogonality principle the stiffness matrix become decoupled for each circumferential harmonic.

The constitutive matrix $\bar{\mathbf{D}}$ in Eq (15) consisting of various integrated shell stiffness: A_{ij}, B_{ij}, D_{ij} and F_{ij}. Shear correction factor equal to 5/6 is used.

The mass matrix is obtained from the kinetic energy of the shell continuum, the kinetic energy is

$$\mathrm{KE} = \frac{\rho}{2}\int_v (\dot{u}^2 + \dot{v}^2 + \dot{w}^2)\,\mathrm{d}V = \frac{\rho}{2}\int_v \{\dot{\mathbf{d}}\}^{\mathrm{T}}\{\dot{\mathbf{d}}\}\mathrm{d}V. \tag{16}$$

Using Eqs. (9) and (10) the kinetic energy will be

$$\mathrm{KE} = \tfrac{1}{2}\mathbf{d}_e^{\mathrm{T}}\mathbf{m}_e\mathbf{d}_e, \tag{17}$$

where $\mathbf{m}_e$ is the element mass matrix given by

$$\mathbf{m}_e = \rho \int_v \mathbf{N}^{\mathrm{T}}\mathbf{N}\,\mathrm{d}V. \tag{18}$$

2.2. Finite element formulation for compressible fluid

A semi-analytical, eight-noded annular ring element is used for discretizing the fluid domain. The governing differential equation for the fluid region is popularly called the wave equation. It denotes the phenomenon in which the energy is propagated by the waves and is applied to problems of sound propagation, sloshing of liquid and fluid–structure interaction. For studying the dynamic analysis of a divergent conical shell conveying fluid velocity potential is the nodal dof. The pressure in excess of hydrostatic pressure, p, is associated with the motion of the fluid. This pressure (p) is given by the Bernoulli's equation.

The following assumptions are made in deriving Eq. (1) the fluid flow is potential, (2) small deformations for the structure, i.e. linear, (3) flow is inviscid, irrotational and isentropic and fluid pressure is normal to the shell wall, (4) fluid is compressible and (5) there is no flow separation or cavitations, (5) the fluid mean velocity distribution is assumed to be constant across a shell section. Further, the velocity potential should satisfy the wave equation shown below:

$$\nabla^2\phi - \frac{1}{c^2}\left(\frac{\partial}{\partial t} + \frac{Q}{A}\frac{\partial}{\partial x}\right)^2\phi = 0, \tag{19}$$

where ϕ is the velocity potential, c the velocity of sound, Q the discharge, A the area of cross-section of the element at the middle. At any given moment the flow (Q) is constant across all the section along the cone. Hence, the average flow velocity in the element is given by

$$U_x = \frac{Q}{A}, \tag{20}$$

where U_x, is the mean axial flow velocity of the fluid:

$$V_x = \frac{Q}{A} + \frac{\partial\phi}{\partial x}, \quad V_\theta = \frac{1}{R}\frac{\partial\phi}{\partial\theta}, \quad V_r = \frac{\partial\phi}{\partial r}. \tag{21}$$

The radial velocity of the fluid must be equal to the instantaneous velocity of the shell. This will satisfy the impermeability or dynamic boundary conditions, which ensures contact between the shell and the fluid. That is

$$V_r = \left.\frac{\partial\phi}{\partial r}\right|_{r=a} = \frac{\partial w}{\partial t} + \frac{Q}{A}\frac{\partial w}{\partial x}. \tag{22}$$

Bernoulli's equation is used to compute the pressure exerted by the fluid on the shell wall. For unsteady flow

$$\frac{\partial\phi}{\partial t} + \frac{1}{2}V^2 + \frac{P}{\rho} = \frac{P_s}{\rho}, \tag{23}$$

where $V^2 = V_x^2 + V_\theta^2 + V_r^2$ and P_s is the stagnation pressure. Now P can be written as the sum of a mean pressure $\bar{P}$ and the perturbation pressure p:

$$P = \bar{P} + p. \tag{24}$$

The nonlinear terms in V^2 are neglected for small deformations we get

$$V^2 \cong \left(\frac{Q}{A}\right)^2 + 2\frac{Q}{A}\frac{\partial\phi}{\partial x}, \tag{25}$$

$$p = -\rho\left(\frac{\partial\phi}{\partial t} + \frac{Q}{A}\frac{\partial\phi}{\partial x}\right). \tag{26}$$

A Galerkin weighted residual approach is used to formulate the finite element form of the governing wave equation in cylindrical coordinates. The result of the manipulations is shown:

$$\int_V N_f^{\mathrm{T}}\left(\nabla^2\phi - \frac{1}{c^2}\left(\frac{\partial}{\partial t} + \frac{Q}{A}\frac{\partial}{\partial x}\right)^2\phi\right)\mathrm{d}V = 0, \tag{27}$$

$$\int_S N_f^{\mathrm{T}}\nabla\phi\cdot\mathbf{n}\,\mathrm{d}S - \int_V \nabla N_f^{\mathrm{T}}\nabla\phi\,\mathrm{d}V - \frac{1}{c^2}\int_V N_f^{\mathrm{T}}\ddot{\phi}\,\mathrm{d}V - \frac{2}{c^2}\int_V N_f^{\mathrm{T}}\frac{Q}{A}\frac{\partial^2\phi}{\partial x\partial t}\,\mathrm{d}V - \frac{1}{c^2}\int_V N_f^{\mathrm{T}}\left(\frac{Q}{A}\right)^2\frac{\partial^2\phi}{\partial x^2}\,\mathrm{d}V = 0, \tag{28}$$

where the weighting function N_f is the fluid shape functions given in Ref. [12]. The variation of velocity potential is expressed in Fourier series in the θ direction. The first term of Eq. (28) is rewritten using the fluid shell interface boundary condition of equation as

$$\int_S N_f^{\mathrm{T}}\nabla\phi\cdot\mathbf{n}\,\mathrm{d}S = \int N_f^{\mathrm{T}}\bar{N}\,\mathrm{d}s\{\dot{U}_e\} + \frac{Q}{A}\int N_f^{\mathrm{T}}\frac{\partial\bar{N}}{\partial x}\,\mathrm{d}S\{U_e\}, \tag{29}$$

where $\bar{N}$ is the w component of the shell shape function and $\mathbf{n}$ the unit normal vector to the structure. Similarly from Eq. (26), the pressure acting on the fluid structure interface can be converted to the finite element equations

$$\int_S \bar{N}^{\mathrm{T}}\rho_f\left(\frac{\partial\phi}{\partial t} + \frac{Q}{A}\frac{\partial\phi}{\partial x}\right)\mathrm{d}S = \rho_f\int_S \bar{N}^{\mathrm{T}}N_f\,\mathrm{d}S\{\dot{\phi}_e\} + \rho_f\frac{Q}{A}\int_S \bar{N}^{\mathrm{T}}\frac{\partial N_f}{\partial x}\,\mathrm{d}S\{\phi_e\}. \tag{30}$$

Now the complete fluid–structure finite element equation is

$$\begin{bmatrix}\mathbf{M}^{uu} & 0\\ 0 & \mathbf{G}^{\phi\phi}\end{bmatrix}\begin{Bmatrix}\ddot{u}\\ \ddot{\phi}\end{Bmatrix} + \begin{bmatrix}0 & \mathbf{C}^{u\phi}\\ -\mathbf{C}^{\phi u} & -\mathbf{C}^{\phi\phi}\end{bmatrix}\begin{Bmatrix}\dot{u}\\ \dot{\phi}\end{Bmatrix} + \begin{bmatrix}\mathbf{K}^{uu} & \mathbf{K}^{u\phi}\\ -\mathbf{K}^{\phi u} & \mathbf{H}^{\phi\phi} - \mathbf{I}^{\phi\phi}\end{bmatrix}\begin{Bmatrix}u\\ \phi\end{Bmatrix} = 0, \tag{31}$$

where

$$\mathbf{m}_e = \rho\int_V\int \mathbf{N}^{\mathrm{T}}\mathbf{N}\,\mathrm{d}V, \quad \mathbf{M}^{uu} = \sum\mathbf{m}_e \quad \text{structural mass matrix}$$

$$\mathbf{G}_e^{\phi\phi} = \frac{1}{c^2}\int_V \mathbf{N}_f^{\mathrm{T}}\mathbf{N}_f\,\mathrm{d}V, \quad \mathbf{G}^{\phi\phi} = \sum\mathbf{G}_e^{\phi\phi} \quad \text{compression energy of fluid,}$$

$$\mathbf{C}_e^{u\phi} = \rho_f\int_S \bar{\mathbf{N}}^{\mathrm{T}}\mathbf{N}_f\,\mathrm{d}S, \quad \mathbf{C}^{u\phi} = \sum\mathbf{C}_e^{u\phi} \quad \text{FSI coupling term}$$

$$\mathbf{C}_e^{\phi u} = \int_S \mathbf{N}_f^{\mathrm{T}}\bar{\mathbf{N}}\mathrm{d}S, \quad \mathbf{C}^{\phi u} = \sum\mathbf{C}_e^{\phi u} \quad \text{FSI coupling term}$$

$$\mathbf{C}_e^{\phi\phi} = \frac{2}{c^2}\int_V\left(\frac{Q}{A}\right)\mathbf{N}_f^{\mathrm{T}}\frac{\partial\mathbf{N}_f}{\partial x}\mathrm{d}V, \quad \mathbf{C}^{\phi\phi} = \sum\mathbf{C}_e^{\phi\phi} \quad \text{coriolis energy of fluid,}$$

$$\mathbf{K}_e^{uu} = \int_V \mathbf{B}^{\mathrm{T}}\bar{\mathbf{D}}\,\mathbf{B}\,\mathrm{d}V, \quad \mathbf{K}^{uu} = \sum\mathbf{K}_e^{uu} \quad \text{structural stiffness matrix,}$$

$$\mathbf{K}_e^{u\phi} = \rho_f\int_S\left(\frac{Q}{A}\right)\bar{\mathbf{N}}^{\mathrm{T}}\frac{\partial\mathbf{N}_f}{\partial x}\mathrm{d}S, \quad \mathbf{K}^{u\phi} = \sum\mathbf{K}_e^{u\phi} \quad \text{stiffness coupling due to flow,}$$

$$\mathbf{K}_e^{\phi u} = \int_S\left(\frac{Q}{A}\right)\mathbf{N}_f^{\mathrm{T}}\frac{\partial\bar{\mathbf{N}}}{\partial x}\mathrm{d}S, \quad \mathbf{K}^{\phi u} = \sum\mathbf{K}_e^{\phi u} \quad \text{stiffness coupling due to flow,}$$

$$\mathbf{H}_e^{\phi\phi} = \int_V \nabla\mathbf{N}_f^{\mathrm{T}}\nabla\mathbf{N}_f\mathrm{d}V, \quad \mathbf{H}^{\phi\phi} = \sum\mathbf{H}_e^{\phi\phi} \quad \text{kinetic energy of fluid,}$$

$$\mathbf{I}_e^{\phi\phi} = \frac{1}{c^2}\int_V\left(\frac{Q}{A}\right)^2\frac{\partial\mathbf{N}_f^{\mathrm{T}}}{\partial x}\frac{\partial\mathbf{N}_f}{\partial x}\,\mathrm{d}V, \quad \mathbf{I}^{\phi\phi} = \sum\mathbf{I}_{\mathrm{e}}^{\phi\phi} \quad \text{centrifugal energy of fluid.}$$

Rewriting the above equation in state-space form by letting $\{a\} = \{u \quad \phi \quad \dot{u} \quad \dot{\phi}\}^{\mathrm{T}}$

$$\lambda \begin{bmatrix} -\mathbf{C}^* & -\mathbf{M}^* \\ \mathbf{M}^* & 0 \end{bmatrix} \{a\} = \begin{bmatrix} \mathbf{K}^* & 0 \\ 0 & \mathbf{M}^* \end{bmatrix} \{a\}, \tag{32}$$

where

$$\mathbf{M}^* = \begin{bmatrix} \mathbf{M}^{uu} & 0 \\ 0 & \mathbf{G}^{\phi\phi} \end{bmatrix}, \quad \mathbf{K}^* = \begin{bmatrix} \mathbf{K}^{uu} & \mathbf{K}^{u\phi} \\ -\mathbf{K}^{\phi u} & \mathbf{H}^{\phi\phi} - \mathbf{I}^{\phi\phi} \end{bmatrix}, \quad \mathbf{C}^* = \begin{bmatrix} 0 & \mathbf{C}^{u\phi} \\ -\mathbf{C}^{\phi u} & -\mathbf{C}^{\phi\phi} \end{bmatrix}.$$

A semi-analytical finite element formulation for compressible flow through shell is formulated. The shell and fluid motion are coupled by the off diagonal terms of the damping and stiffness matrices. For stationary fluids the coupling in stiffness vanishes. The equation is converted to state-space form Eq. (32) is solved for the eigenvalues using LAPACK routine, DGEGV [13].

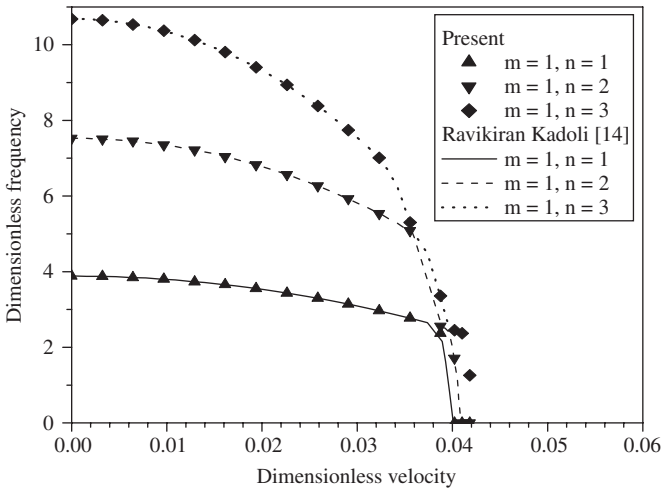

Fig. 4. Validation of the result obtained from the present study with that of Ravikiran Kadoli [14]. Shell condition is made of mild steel, $l/a = 5.21$, $a/h = 584$ and clamped–clamped boundary.

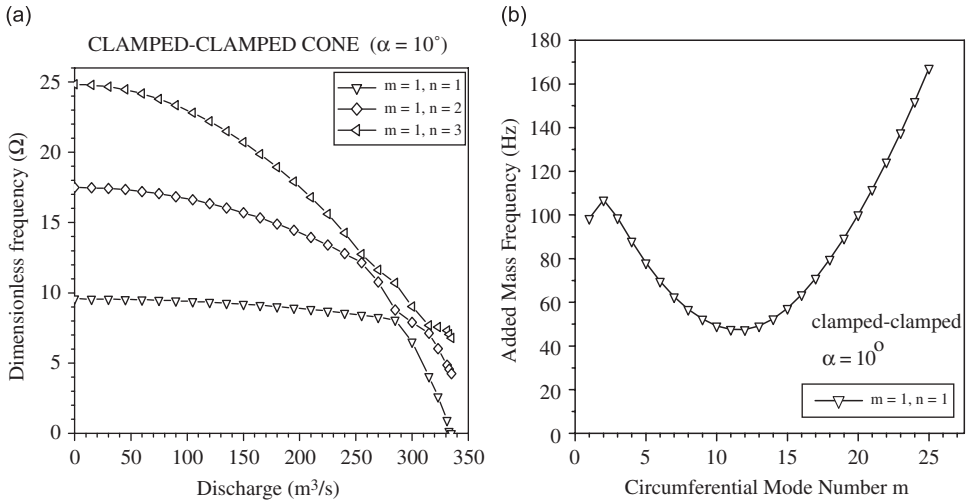

Fig. 5. (a) Variation of the dimensionless frequency (Ω) with respect to discharge (Q) for water flowing through conical shell of vertex angle $\alpha = 10^\circ$ with $l/a = 1.04$ $a/h = 584$ for clamped–clamped boundary condition. (b) Circumferential mode versus natural frequency of fluid filled conical shell, for $l/a = 1.0438$ and $a/h = 584$.

3. Validation

In the present study, the computer code is developed for a conical shell conveying fluid, appropriately accounting for variation of mean velocity along the cone. Owing to non-availability of literature on conical shells conveying fluid, it was felt that the formulation could be validated by making comparison between the results obtained from the present code for cylinder ($\alpha = 0^\circ$), and those reported by Ravikiran Kadoli [14]

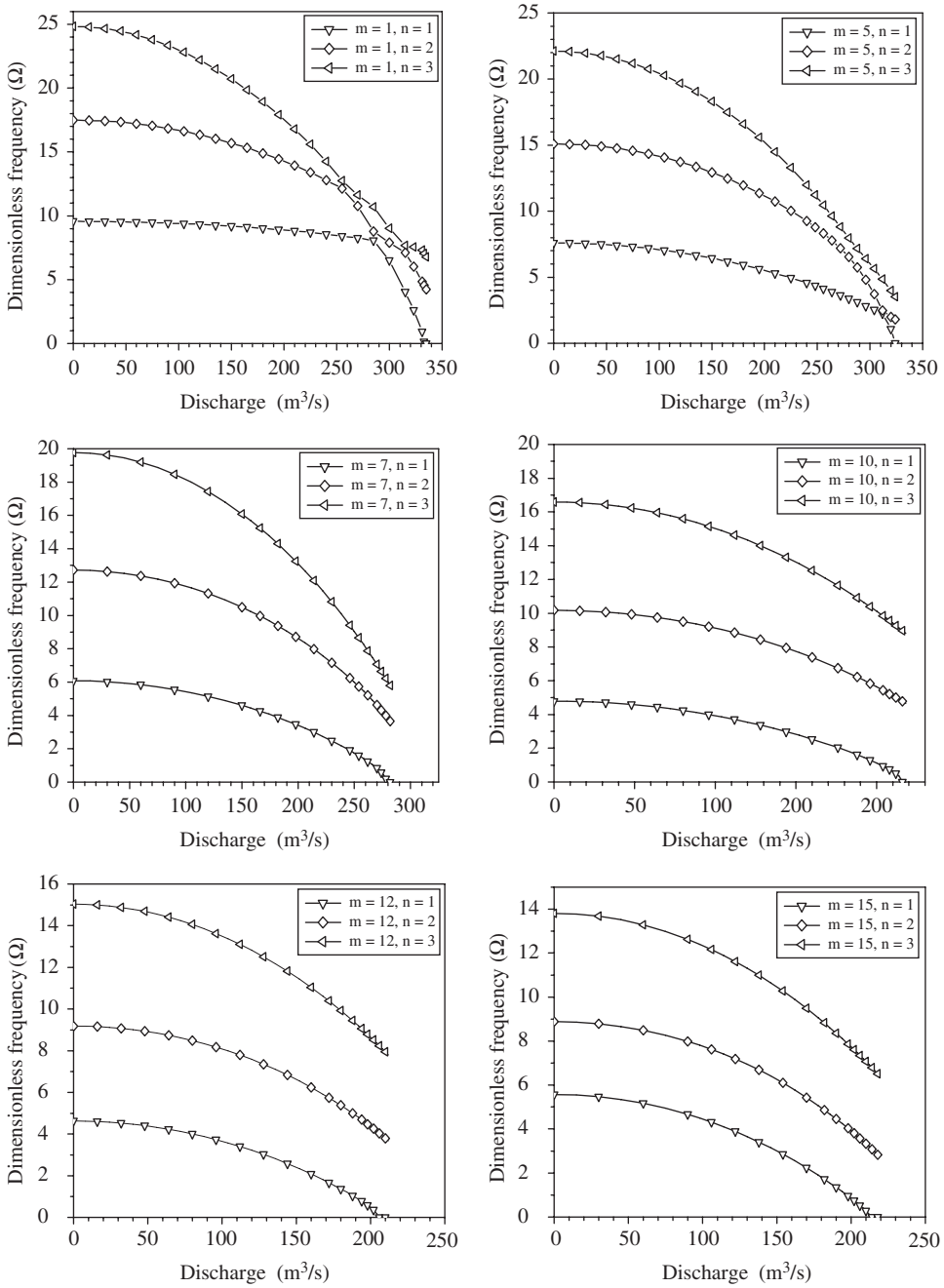

Fig. 6. Variation of dimensionless frequency (Ω) with respect to discharge (Q) for water flowing through the conical shell of vertex angle $\alpha = 10^\circ$ with $l/a = 1.04$, $a/h = 584$, $m = 1$, 5, 7, 10, 12 and 15, for clamped–clamped boundary condition.

who has studied the behavior of cylindrical shell conveying fluid. Shell is made up of mild steel with $l/a = 5.21$, $a/h = 584$ and clamped–clamped boundary condition. The study has been carried out for first circumferential modes for various axial modes. The variation of dimensionless frequency versus dimensionless velocity has been compared in Fig. 4 for the first three axial modes associated with circumferential harmonics 1. There is a very good correlation between results of present study and that of Ravikiran Kadoli [14].

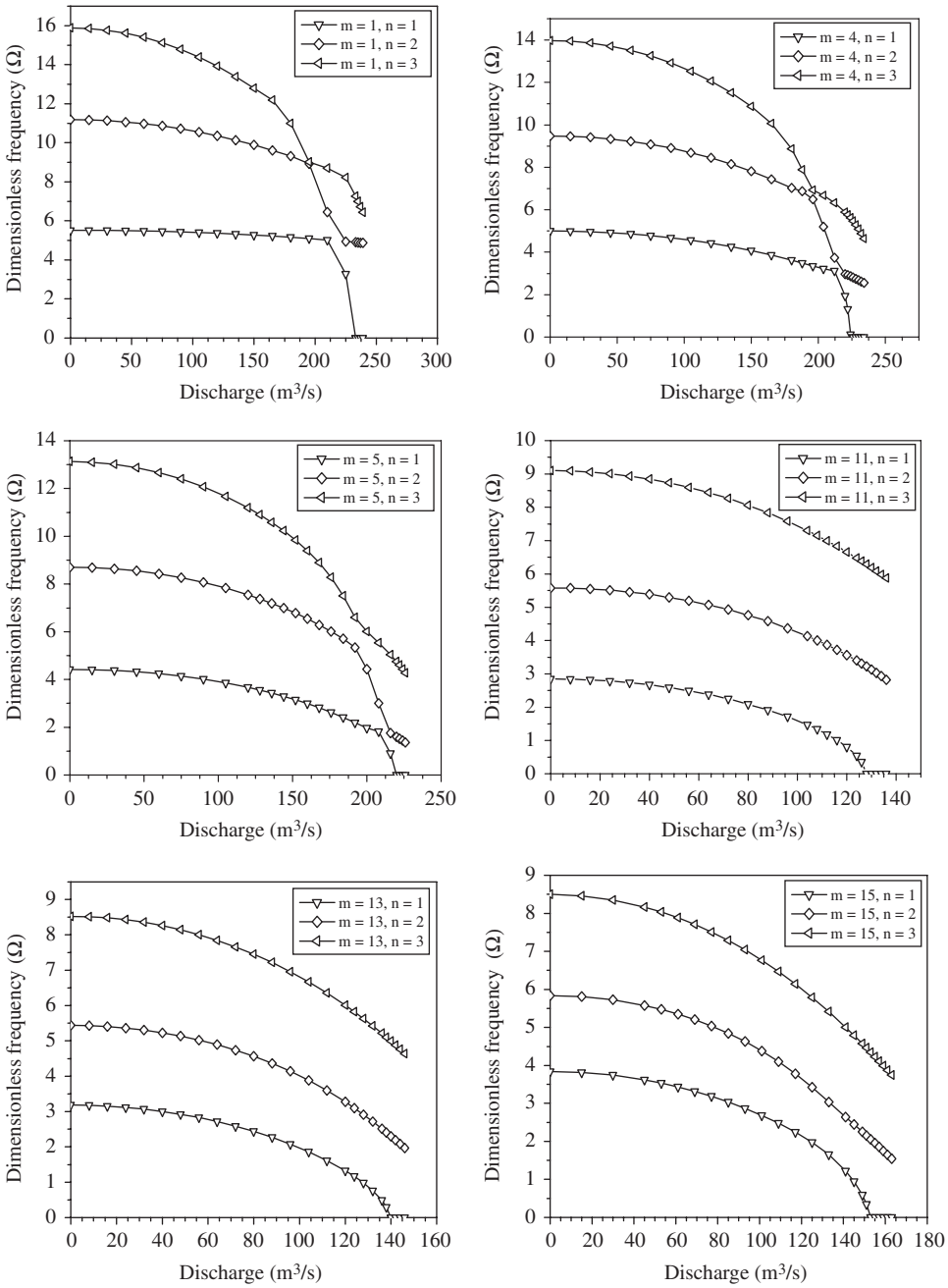

Fig. 7. Variation of dimensionless frequency (Ω) with respect to discharge (Q) for water flowing through the conical shell of vertex angle $\alpha = 30^\circ$ with $l\,a = 1.04$, $a/h = 584$, $m = 1$, 4, 5, 11, 13 and 15, for clamped–clamped boundary condition.

4. Results and discussion

4.1. Instability studies on clamped–clamped shell

The main objective of the present study is to establish a correlation between the critical discharge and the natural frequency characteristics of the conical shells conveying fluid. An attempt is made to compare the behavior of conical and cylindrical shells. In order to compare the instability behavior of conical shell with

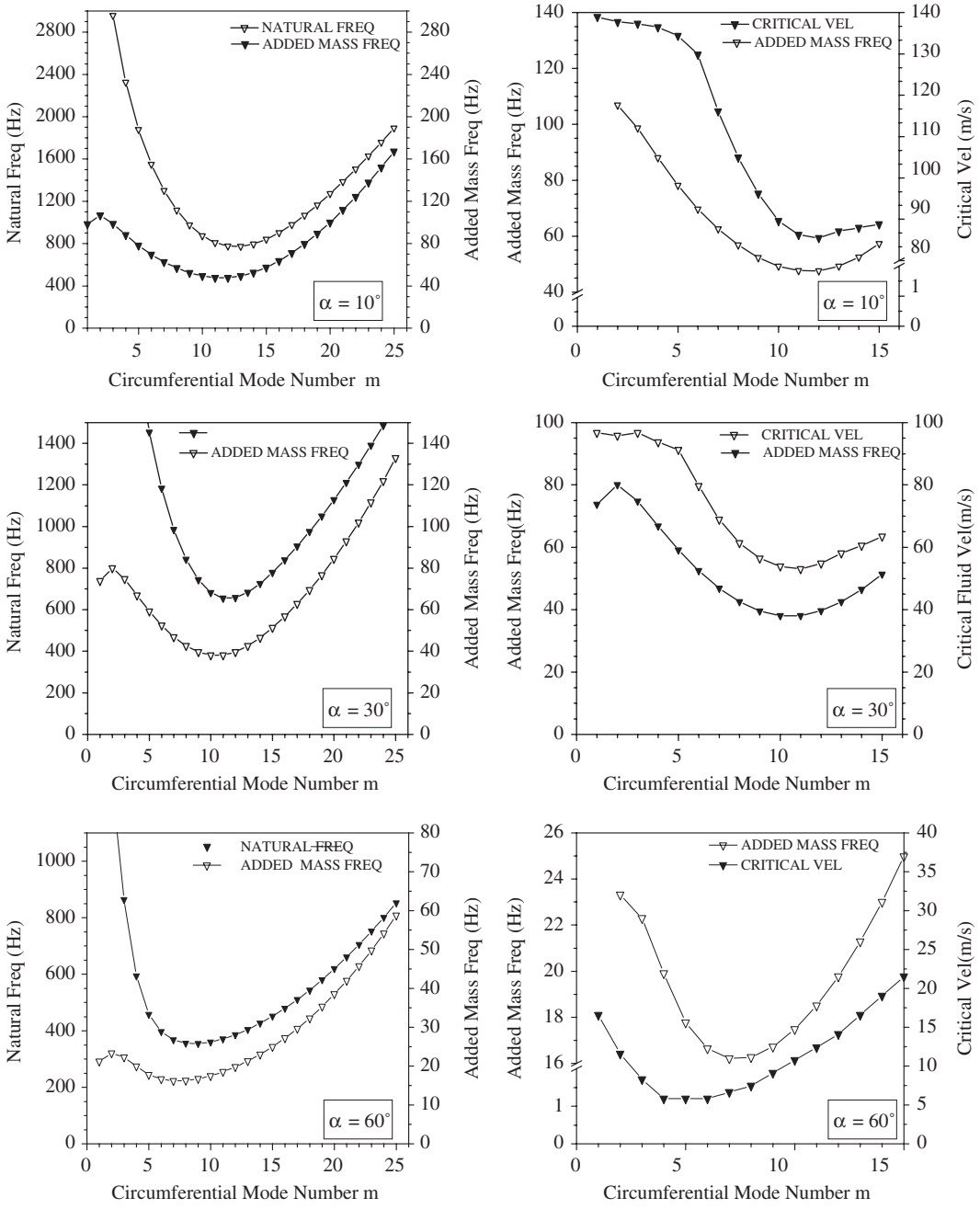

Fig. 8. Frequencies (Hz) and critical velocities (m/s) of mild steel conical shell for different vertex angle ($\alpha = 10^\circ, 30^\circ, 60^\circ$), with $l/a = 1.04$, $a/h = 584$, clamped–clamped boundary condition.

that of equivalent cylinder shell, critical discharge value (Q_{cri}) is divided by the middle cross-sectional area of the cone, which gives critical velocity (U_{cri}). For a conical shell of middle radius 0.876 m (a), length 0.9144 m (l), vertex angle 10°(α) and thickness 1.5 mm (t) geometry, with clamped–clamped boundary condition is studied. Twenty circumferential modes ($m = 1$–20) and the corresponding three axial modes ($n = 1, 2, 3$) are calculated. It is noticed that the real eigenvalue decrease as the flow discharge increases and vanishes at critical discharge (divergence-type instability). Further, the study is made for different cone vertex angle like 30°, 60°. Eigenvalues obtained are expressed in dimensionless quantities as $\Omega = (\omega/\omega_o) \times 100$, where $\omega_o = U_o/r_s$, ω is the real natural frequency, r_s is the small end radius of the shell, and $U_o = \sqrt{E_o/\rho_s}$, in which ρ_s is the density of the shell material and E_0 is the Young's modulus of the shell material.

The variation of flow discharge (Q) with dimensionless frequency (Ω) has been shown in Fig. 5(a). In general, the buckling of shells is a complicated phenomenon and depending upon the type of loading, boundary condition and parameters of the shell, it may occur at different circumferential modes. Divergence buckling may perhaps be categorized as static buckling. An attempt is being made to correlate the buckling behavior of the shells and the natural frequencies of the shell with respect to circumferential mode. To this end the frequency characteristics of different shells were obtained (without flow). Fig. 5(b) shows the plot of natural frequency as a function of circumferential mode for $l/a = 1.0438$ and $a/h = 584$, vertex angle ($\alpha = 10°$) for clamped–clamped boundary condition.

In addition, a detailed study was made on the instability behavior of different shells for all circumferential modes. Some of the results are presented in Figs. 6 and 7. From this study, the circumferential mode pertaining to the lowest critical discharge was identified and from the Fig. 8, it is found that there is a clear correlation between the circumferential buckling modes of shells conveying fluids and the circumferential mode at which the lowest natural frequency occurs for the fluid-filled shell.

The correlation is due to the fact that buckling mode will be related to stiffness of the conical shell and the mode which has lowest frequency would be likely to buckle first, as its stiffness is lower. But in the case of cone with vertex angle $\alpha = 60°$, there is shift in the circumferential buckling mode from the circumferential mode at which the lowest natural frequency occurs for the fluid-filled shells.

Results are summarized in Table 1. It is inferred that there is a good correlation between the circumferential mode at which the lowest critical discharge occurs and the circumferential mode at which the shell has got the lowest frequency.

A similar study for other boundary conditions such as clamped free and simply supported are described in the next section.

4.2. Instability studies on clamped–free and simply supported shell

Study has been carried out on shells with simple supported boundary condition. The present study examines the influence of flow discharge on the natural frequency characteristics of conical shell of $l/a = 1.04$, $a/h = 584$, under simply supported boundary condition. Initially, the frequency characteristics of different shells were obtained (without flow). Variation of dimensionless frequency with discharge for different circumferential mode has been shown in Fig. 9. A similar work was carried out for clamped–free boundary condition (Figs. 10–14). From Fig. 13, it is found that the same correlation repeats for clamped–free for boundary condition. It is found that the above correlation is applicable to all boundary conditions in general.

Table 1
Comparison of circumferential mode having the lowest natural frequency for the fluid-filled shell and that of circumferential buckling mode of conical shell conveying fluid in clamped–clamped boundary condition

Boundary condition	Case (mild steel) $l/a = 1.04$, $a/h = 584$. Cone angle (α) (deg)	Circumferential mode at which the lowest natural frequency occurs	Circumferential mode at which the buckling occurs
CC	10	12	12
	30	10	11
	60	7	5 or 6

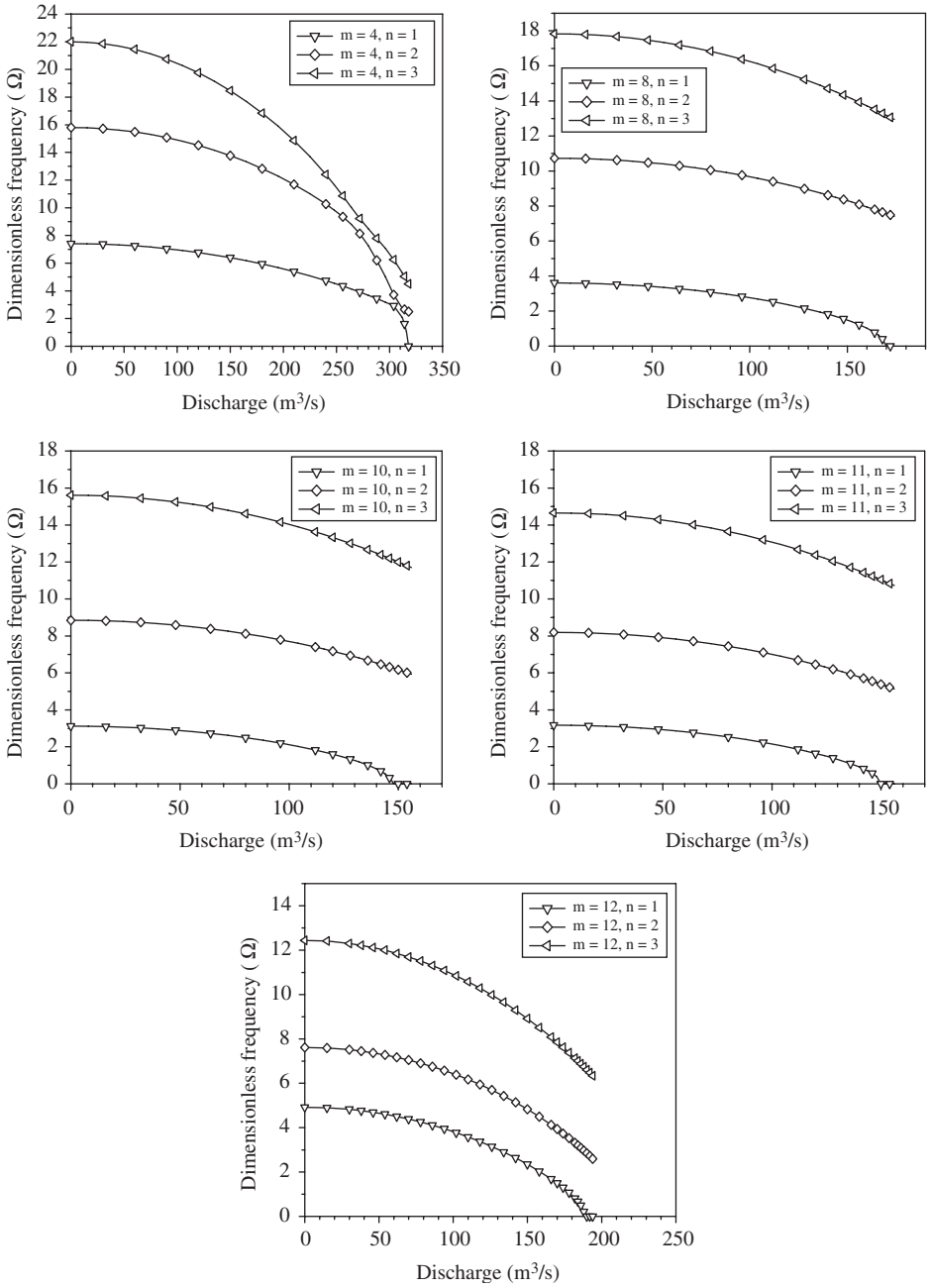

Fig. 9. Variation of dimensionless frequency (Ω) with respect to discharge (Q) for water flowing through the conical shell of vertex angle $\alpha = 10^{\circ}$ with $l/a = 1.04$, $a/h = 584$, for simple supported boundary condition.

This may due to the fact that the stiffness of the shell for that particular circumferential mode which buckles earlier is the least (Fig. 14).

Results are summarized in Table 2 and 3. From Table 2, it is observed that there is a good correlation between the circumferential mode at which the lowest critical discharge occurs and the circumferential mode at which the shell has got the lowest frequency. From the table, it is very clear that the correlation is true for all cases.

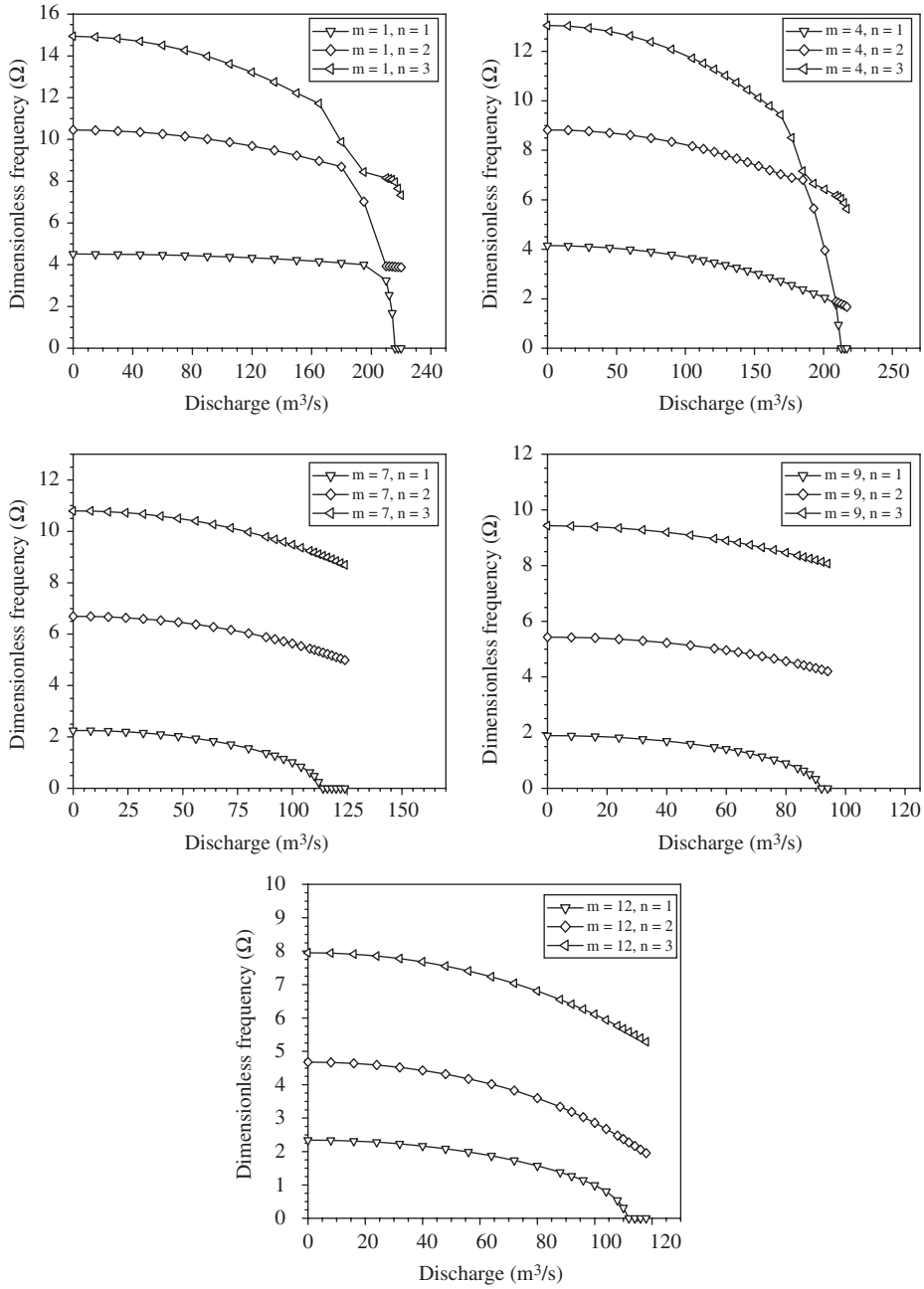

Fig. 10. Variation of dimensionless frequency (Ω) with respect to discharge (Q) for water flowing through the conical shell of vertex angle $\alpha = 30^\circ$ with $l/a = 1.04$,$a/h = 584$, for simple supported boundary condition.

4.3. Comparison of dynamic behavior of conical and cylindrical shell

In order to compare the dynamic behavior of cylindrical and conical shells conveying fluid, the cross-sectional area of the shell at half the length, l/a and a/h ratio has been taken same for both the shell. In the case of cone critical discharge (Q_{cri}) value is divided by the middle cross-sectional area of the cone will give the critical velocity value (U_{cri}). For various shells considered the critical velocity value for various circumferential modes are tabulated in Table 4. It has been found earlier that there is a clear correlation between the

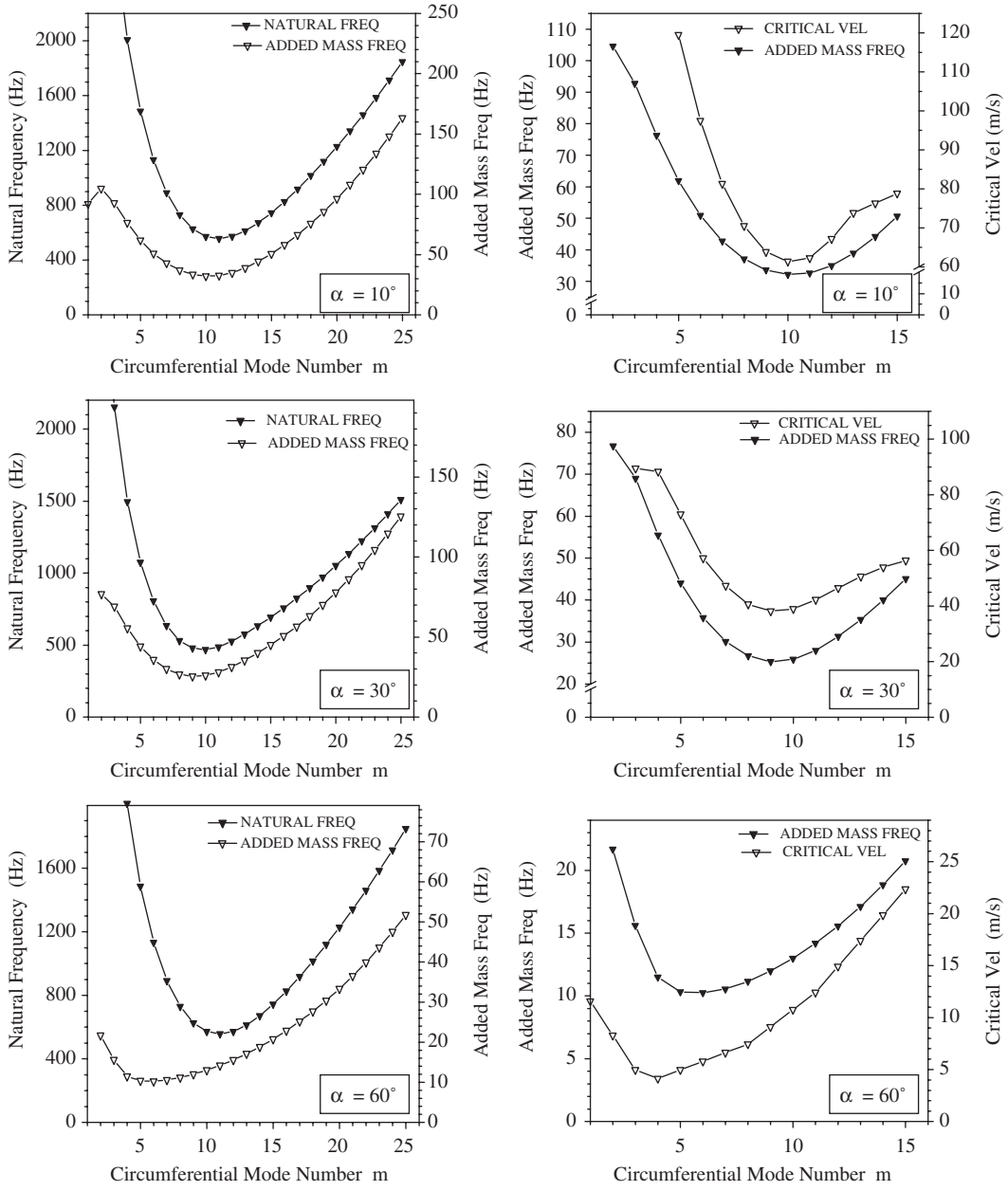

Fig. 11. Frequencies (Hz) and critical velocities (m/s) of mild steel conical shell for different vertex angle ($\alpha = 10^\circ$, 30°, 60°), with $l/a = 1.04$, $a/h = 584$, simple supported boundary condition.

circumferential buckling modes of shells conveying fluids and the circumferential mode at which the lowest natural frequency occurs for the fluid-filled shell. In addition to that, it is seen that as the vertex angle increases the circumferential buckling mode as well as critical velocity value of that mode also comes down. For example in Table 4, results are given for different shell under clamped–clamped boundary condition. For cylinder the circumferential buckling mode (12,1) the critical velocity value is 91.26 m/s. As vertex angle increased to 60°, corresponding circumferential buckling mode (5–7,1) the critical velocity value is 6.64 m/s.

A similar work was carried out for clamped–free and simple supported boundary condition. From Tables 5 and 6, it is found that the same observation repeats for clamped–free and simple supported boundary

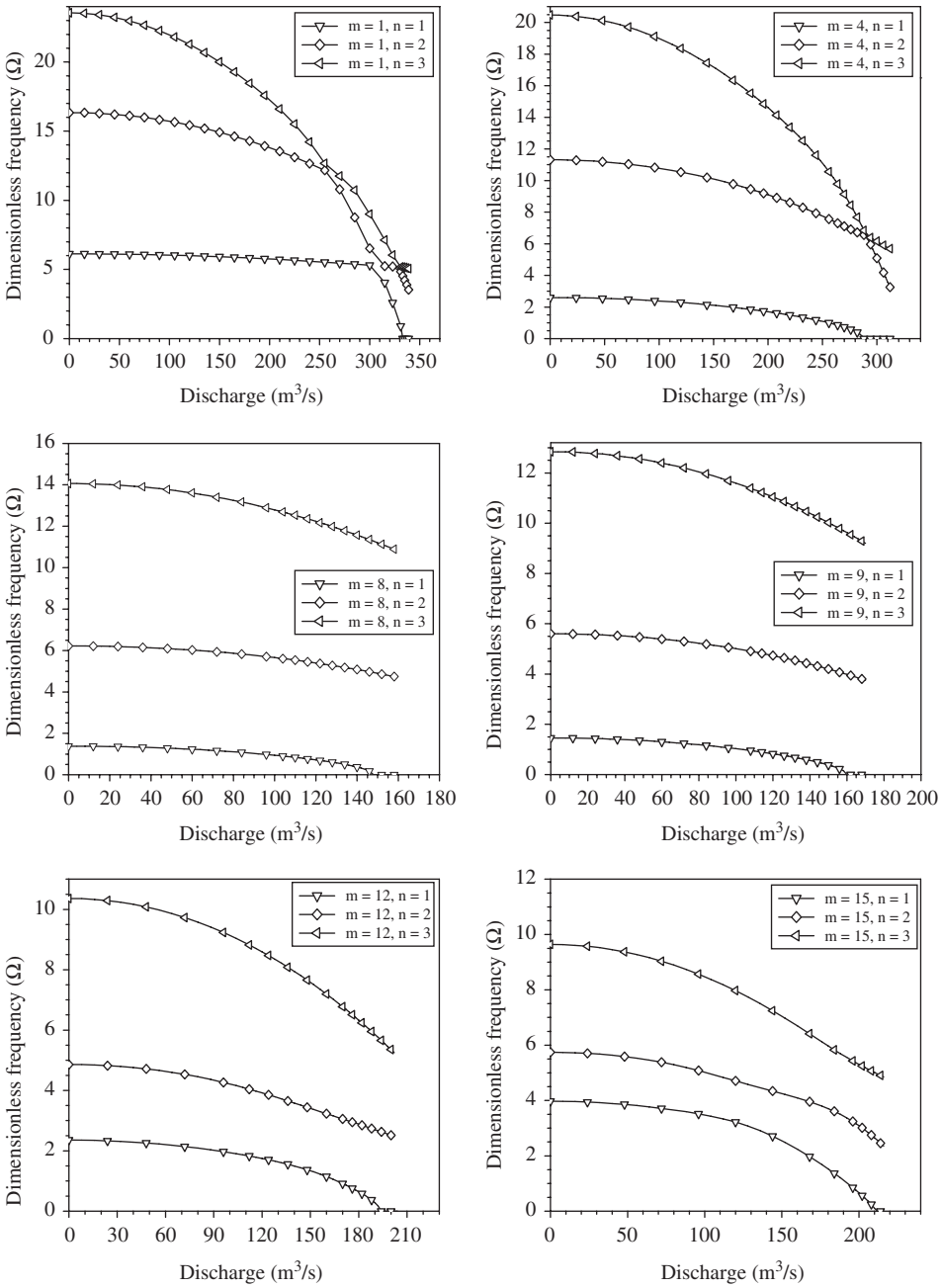

Fig. 12. Variation of dimensionless frequency (Ω) with respect to discharge (Q) for water flowing through the conical shell of vertex angle $\alpha = 10^\circ$ with $l/\alpha = 1.04$, $a/h = 584$, $m = 1$, 4, 8, 9, 12 and 15, for clamped–free boundary condition.

condition. In general, critical velocity value decreases drastically if vertex angle is increased for all boundary condition.

5. Conclusion

Conical shells conveying fluid find application in specific engineering fields. In the present study, the dynamic analysis of conical shells conveying fluid has been studied by using semi-analytical finite element

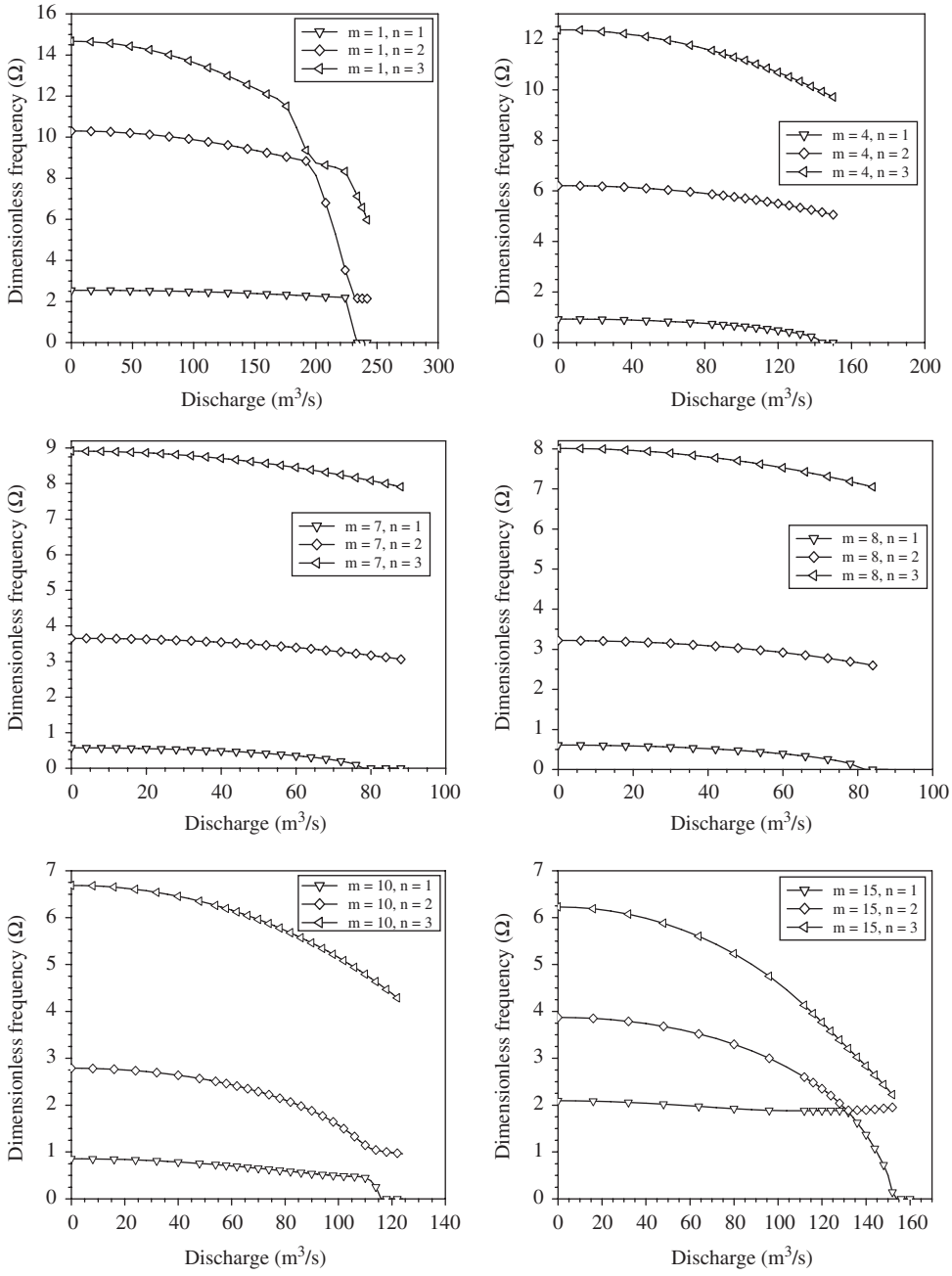

Fig. 13. Variation of dimensionless frequency (Ω) with respect to discharge (Q) for water flowing through the conical shell of vertex angle $\alpha = 30^\circ$ with $l/\alpha = 1.04$, $a/h = 584$, $m = 1$, 4, 7, 8, 10 and 15, for clamped–free boundary condition.

procedure. The study has been carried out shells having different cone angles. The behaviors of conical shells have been compared with that of cylindrical shells. The following are the conclusion base on the present study:

1. There is a correlation between circumferential buckling mode of shells conveying fluid and the circumferential mode at which the lowest frequency occurs for fluid-filled shells.
2. It is seen that as the vertex angle increases the circumferential buckling mode as well as the critical velocity value of the mode also comes down.

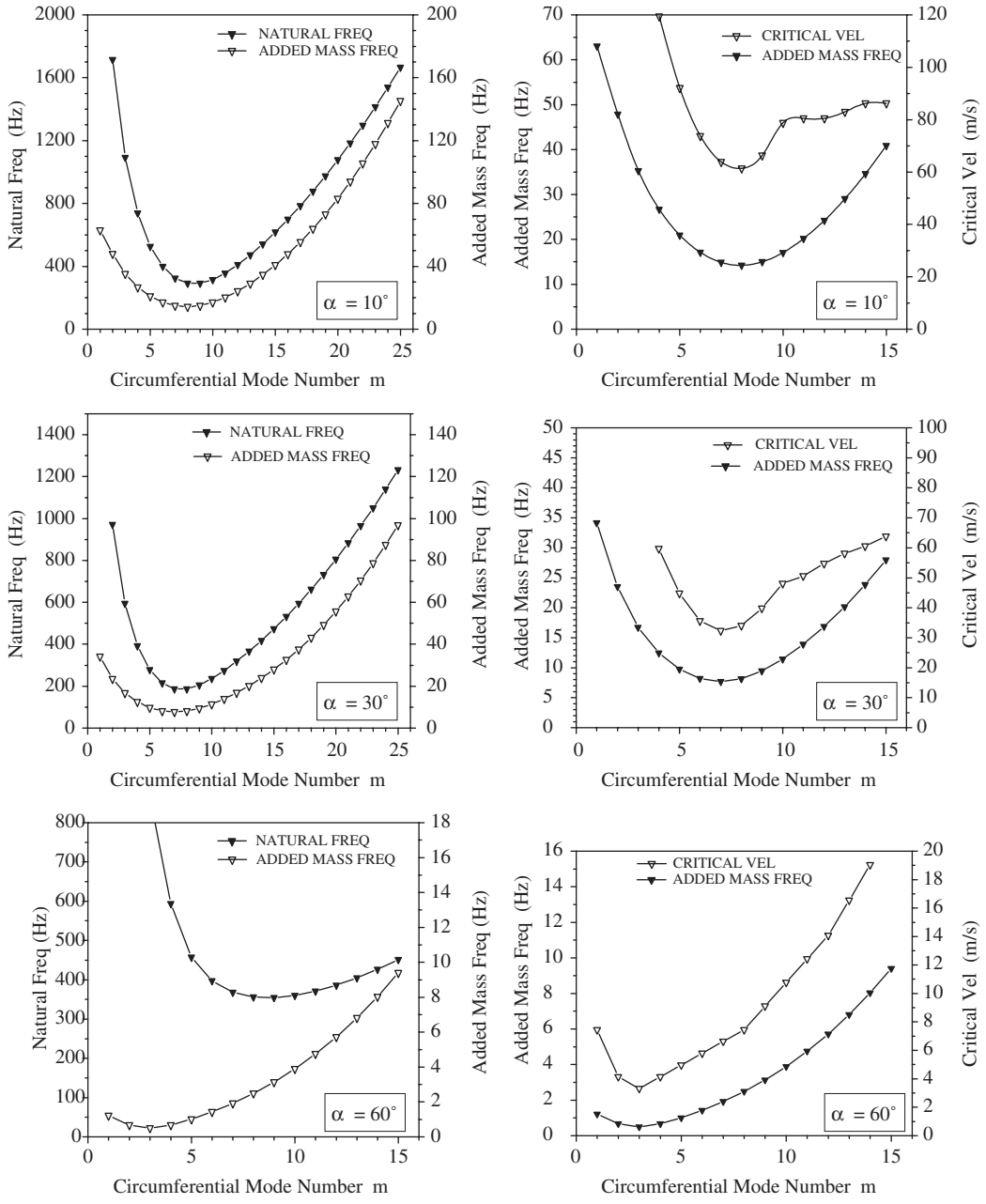

Fig. 14. Frequencies (Hz) and critical velocities (m/s) of mild steel conical shell for different vertex angle ($\alpha = 10^\circ$, 30°, 60°), with $l/a = 1.04$, $a/h = 584$, clamped–free boundary condition.

Table 2
Comparison of circumferential mode having the lowest natural frequency for the fluid-filled shell and that of circumferential buckling mode of conical shell conveying fluid in simple supported condition

Boundary condition	Case (mild steel) $l/a = 1.04$, $a/h = 584$. Cone angle (α) (deg)	Circumferential mode at which the lowest natural frequency occurs	Circumferential mode at which the buckling occurs
SS	10	10	10
	30	9	9
	60	7	4

Table 3
Comparison of circumferential mode having the lowest natural frequency for the fluid-filled shell and that of circumferential buckling mode of conical shell conveying fluid in clamped–free boundary condition

Boundary condition	Case (mild steel) $l/a = 1.04$, $a/h = 584$. Cone angle (α) (deg)	Circumferential mode at which the lowest natural frequency occurs	Circumferential mode at which the buckling occurs
CF	10	8	8
	30	7	7
	60	3	3

Table 4
Critical velocity value for vertex angle $\alpha = 0^\circ$, 10°, 30°, 60° under clamped–clamped boundary condition

Circumferential mode number (m)	Critical flow velocity (U_{cri}), for cone vertex angle (α) clamped–clamped boundary condition			
	Cylinder ($\alpha = 0^\circ$)	$\alpha = 10^\circ$	$\alpha = 30^\circ$	$\alpha = 60^\circ$
1	148.5	138.96	96.65	16.59
3	147.26	137.3	96.65	9.96
5	145.6	134.4	91.25	6.64
7	124.03	116.15	68.85	6.64
10	96.65	89.59	53.92	11.614
12	91.26	85.45	54.75	14.93
15	92.92	88.77	63.45	23.23

Table 5
Critical velocity value for vertex angle $\alpha = 0^\circ$, 10°, 30°, 60° under clamped–free boundary condition

Circumferential mode number (m)	Critical flow velocity (u_{cri}), for cone vertex angle (α) clamped–free boundary condition			
	Cylinder ($\alpha = 0^\circ$)	$\alpha = 10^\circ$	$\alpha = 30^\circ$	$\alpha = 60^\circ$
1	148.5	138.1	97.06	7.46
3	147.67	137.7	84.62	3.32
5	114.49	92.08	44.79	4.97
7	82.96	63.87	32.35	6.64
8	80.47	61.39	34	7.45
10	89.6	78.81	48.12	10.77
15	91.2	87.93	63.87	21.53

Table 6
Critical velocity value for vertex angle $\alpha = 0^\circ$, 10°, 30°, 60° under simple supported boundary condition

Circumferential mode number (m)	Critical flow velocity (u_{cri}), for cone vertex angle (α) simple supported boundary condition			
	Cylinder ($\alpha = 0^\circ$)	$\alpha = 10^\circ$	$\alpha = 30^\circ$	$\alpha = 60^\circ$
1	147.67	133.98	89.59	11.62
3	146.84	133.15	89.57	4.98
4	145.6	131.9	88.33	4.14
7	87.11	81.30	47.29	6.63
9	68.86	63.87	38.15	9.13
10	65.54	61.39	38.98	10.77
15	82.55	78.81	56.41	22.39

References

[1] R. Ramasamy, N. Ganesan, Finite element analysis of fluid filled isotropic cylindrical shells with constrained viscoelastic damping, *Computers & Structures* 70 (1998) 363–376.
[2] Jayaraj Kochupillai, N. Ganesan, Chandramouli Padmnabhan, A semi-analytical coupled finite element formulation for composite shells conveying fluids, *Journal of Sound and Vibration* 258 (2) (2002) 287–307.
[3] M.P. Païdoussis, G.X. Li, Pipes conveying fluid: a model dynamical problem, *Journal of Fluids and Structures* 7 (1993) 137–204.
[4] M.P. Païdoussis, *Fluid– Structure Interactions 1998: Slender Structures and Axial Flow*, Vol. I, Academic Press, London, 1998.
[5] D.J. Wilkins Jr., C.W. Bert, D.M. Egle, Free vibrations of orthotropic sandwich conical shells with various boundary conditions, *Journal of Sound and Vibration* 13 (1970) 211–228.
[6] A. Selman, A.A. Lakis, Vibration analysis of anisotropic open cylindrical shells subjected to flowing fluid, *Journal of Fluids and Structures* 11 (1997) 111–134.
[7] Jeng-Shian Chang, Wen-Jiann Chiou, Natural frequencies and critical velocities of fixed–fixed laminated circular cylindrical shells conveying fluids, *Computers & Structures* 57 (5) (1995) 929–939.
[8] G.C. Everstine (Ed.), A symmetric potential formulation for fluid–structure interaction. Letter to the Editor, *Journal of Sound and Vibration* 79 (1981) 157–160.
[9] A.A. Lakis, P. Van Dyke, H. Ouriche, Dynamic analysis of anisotropic fluid-filled conical shells, *Journal of Fluids and Structures* 6 (1992) 135–162.
[10] R.M. Jones, *Mechanics of Composite Materials*, second ed., Taylor & Francis Inc., Philadelphia.
[11] C. Decolon, *Analysis of Composite Structures*, Hermes Penton Science, London, 2002.
[12] C.T.F. Ross, *Pressure Vessels under External Pressure: Statics, Dynamics*, Elsevier, London, 1994.
[13] G.H. Golub, C.F. Van Loan, *Matrix Computations*, third ed., Johns Hopkins University Press, Baltimore, MD, 1996.
[14] Ravikiran Kadoli, Studies on Shells of Revolution under Thermal Environment, PhD Thesis, Indian Institute of Technology, Madras, 2003.